... a nonexclusive royalty free license in and to any copyright covering the article

CONF-800850--2

# DEUTERIUM PROFILEMETRY AND DIFFUSION COEFFICIENT IN ELECTROCHARGED STAINLESS STEEL*

MASTER

M. B. Lewis and K. Farrell
Metals and Ceramics Division
Oak Ridge National Laboratory
Oak Ridge, Tennessee 37830

The method of nuclear microanalysis using the reaction D(d,p)T is used to measure concentration-depth profiles of deuterium in austenitic type 310 stainless steel electrocharged in 1 N $D_2SO_4$ with arsenic poison at room temperature. The influence of aging after charging is examined. A near-surface density of 0.6 deuterium atoms per metal atom (i.e., 38 at. %) is found for the initially charged condition. Associated with this high gas concentration is considerable microstructural damage. An analysis of the deuterium depth profiles yields a room-temperature diffusion coefficient for deuterium of $1.4 \times 10^{-16}$ $m^2s^{-1}$ at high concentrations which is consistent with extrapolation of higher-temperature data available from other techniques for annealed material. At lower deuterium concentrations, $<10^{-2}$, in the aged material the extracted diffusion coefficient is a factor of three higher, implying a dependence on concentration. At concentrations $<10^{-3}$, diffusion may be hindered by dislocation trapping.

DISCLAIMER

This book was prepared as an account of work sponsored by an agency of the United States Government. Neither the United States Government nor any agency thereof, nor any of their employees, makes any warranty, express or implied, or assumes any legal liability or responsibility for the accuracy, completeness, or usefulness of any information, apparatus, product or process disclosed, or represents that its use would not infringe privately owned rights. Reference herein to any specific commercial product, process, or service by trade name, trademark, manufacturer, or otherwise, does not necessarily constitute or imply its endorsement, recommendation, or favoring by the United States Government or any agency thereof. The views and opinions of authors expressed herein do not necessarily state or reflect those of the United States Government or any agency thereof.

* Research sponsored by the Division of Materials Sciences, U.S. Department of Energy under contract W-7405-eng-26 with the Union Carbide Corporation.

M. B. Lewis 1 10

## Introduction

In hydrogen embrittlement and hydriding studies of metals, the hydrogen is frequently introduced by cathodic charging in aqueous acid solution. Usually a poison such as arsenic or sulfide ions is added to the electrolyte to boost hydrogen uptake (1). Under these conditions it is expected that the hydrogen concentration in the surface layers of the cathode will be large in accordance with the expectedly very high fugacity of hydrogen at the surface. Once absorbed, ingress of hydrogen proceeds by diffusion, the rate of which may be different from that measured for the usual gas permeation conditions because of hydrogen-hydrogen interaction imposed by the high concentration of hydrogen, and from trapping or pipe diffusion at microstructural damage (2–8) cointroduced during charging. Knowledge of the hydrogen concentrations and diffusion associated with cathodic charging is therefore needed to provide a better understanding of hydrogen behavior in metals. We have measured these parameters for an austenitic stainless steel cathodically charged in a poisoned electrolyte.

## Procedure

Specimens were cathodically hydrogenated and their concentration profiles were determined by nuclear microanalysis using a probing beam of ions from a particle accelerator. Details of the principles and practice of this technique are available elsewhere (9–11). The particular conditions used in the present experiments are described in Ref. 10. Briefly, a monoenergetic beam of ions impinges at a known angle on a target surface where it penetrates the surface and undergoes a nuclear reaction with the impurity in the target. The reaction products are scattered and a fraction of them are emitted from the target and captured in a detector which measures the yield of reaction ions, Y(E), and their energy, E. The yield is related to the concentration, C, of the specific target element, and their emergent energy is a function of the depth, x, at which the nuclear reaction occurred. Thus, a concentration-depth, $C_x$, profile can be obtained. The depth of measurement of the profile is limited to the penetration of the probing ion (of the order of 1 μm in the present studies). If the target element is mobile, the shape of the profile will change with time and temperature, and small shifts of less than 0.1 μm are readily detected; analyses of these shifts in terms of Fick's diffusion laws gives an effective diffusion coefficient.

We used deuterium instead of hydrogen in order to utilize the well-characterized D(d,p)T reaction, where D denotes the target atom, d the probe ion, and p and T the measured reaction products. The targets were 5-mm diam disks, 0.3 mm thick, of type 310 stainless steel (21.1 wt % Ni, 23.4 Cr, 2.1 Mn, 1.0 Si, 0.06 C) annealed at 1050°C in helium. Four disks were mechanically polished on Syntron lapping wheels to a 0.1 μm diamond finish and were spot welded on their edges to a cross of nickel wires. This assembly was suspended in the electrolyte such that the polished face of each disk was equidistant from a surrounding cylindrical platinum anode. The electrolyte was 1 N $D_2SO_4$ poisoned with 2.5 g metallic arsenic per cubic meter.* The bath was maintained at 24°C and was stirred gently with a plastic-coated magnetic paddle. The DC current density was 1 kA $m^{-2}$ at 3 V, and the charging time was 6 ks.

*With no arsenic in the electrolyte, deuterium uptake in the cathode is significantly reduced.

Immediately after electrocharging, the specimens were washed in water and alcohol. One was quickly transferred to the ion scattering chamber which was then pumped to a pressure of less than $10^{-3}$ Pa to allow accurate energy and particle current measurements. The minimum time between cessation of charging and beginning of probing was usually 480 s. The time required for analysis was 60 to 300 s. The remaining specimens were allowed to age for periods up to several hours at room temperature and pressure. For specimens that were probed twice during the experiment, care was taken to insure that the beam spots never overlapped in order to avoid defects introduced by the ion beam from affecting deuterium egress (10). While defects are introduced during measurement, the measuring time is too short to affect the results.

## Data Analysis and Results

The data from the nuclear reactions are pulses or counts (yield) per measurement channel (energy) and are stored in a computer. They must be converted to concentration-depth data which are then analyzed through suitable diffusion expressions to obtain diffusion coefficients.

### Concentration-Depth Profiles

Simple concentration-depth data, $C_x$, are derived from the yield-energy data by the method of convolution integrals (12). A computer code estimates energy losses, straggling, multiple scattering, and other relevant kinematic information then calculates the convolution integrals

$$Y(E)/\Delta E = K\int_S P_{in} C_x b P_{out} dS \qquad (1)$$

where $Y(E)/\Delta E$ = the yield of reaction product,
$K$ = the normalizing constant including beam flux on the target,
$P$ = the Gaussian functions whose widths are determined by the overall resolution,
$b$ = the nuclear reaction cross section, and
$S$ = the space of energy and volume over which the reaction takes place.

The stopping powers are taken from Ref. 13, and Bragg's rule (9) is used to estimate stopping powers in the target. Cross sections are given by Ref. 14. To extract $C_x$, an analytic form for $C_x$, such as the error function, may be chosen and the appropriate error function parameter from Eq. (1) may be adjusted to fit the $Y(E)/\Delta E$ data. Alternatively, $C_x$ may be factored out and solved for directly via a deconvolution procedure.

For the above analytic method, the gas distribution is assumed to be described by the usual diffusion laws such that the profiles should follow the aging pattern depicted schematically in Fig. 1. Here the boundary condition assumed during charging is

$$C = C_o \text{ for } x = 0, t_i > 0 , \qquad (2)$$

where C is the concentration (expressed throughout this work as gas atoms per metal atom) and $t_i$ is the charging or ingress time. The solution for Fick's laws satisfying this condition would then be

$$C(x,t_i) = C_o \operatorname{erfc} [x/2(Dt_i)^{1/2}] , \qquad (3)$$

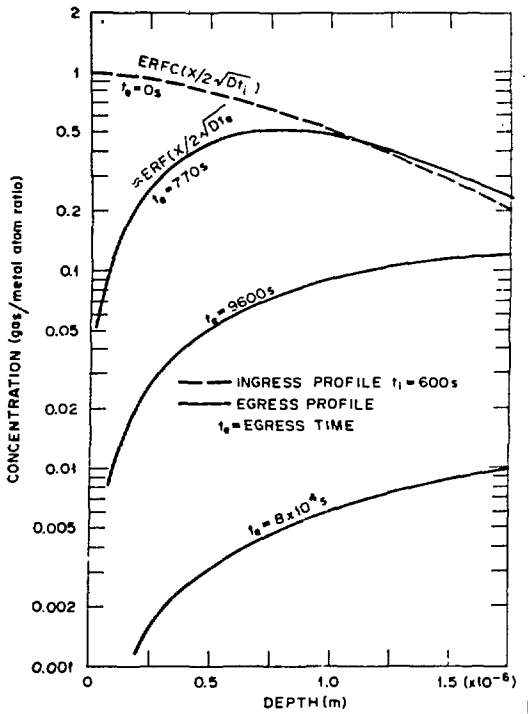


Fig. 1 - Schematic illustration of expected concentration profiles near the specimen surface at points in time during electrocharging and three points in time during release (decay) after a fixed electrocharging time.

during the electrocharging process, where D is the diffusion coefficient and x is the distance below the surface along the surface normal. As can be seen in Fig. 1, if the charging time is long compared to the time for release or egress, the region near the specimen surface can be assumed relatively uniform in concentration $C_o$ when the charging ends (i.e., when the specimen is removed from the electrolytic bath). This point in time becomes $t_e = 0$ for the process of deuterium egress with boundary conditions

$$C = C_o \text{ for } t_e = 0; \qquad C = 0 \text{ for } x = 0, t_e > 0 , \tag{4}$$

for which the solution satisfying Fick's laws is

$$C(x,t_e) = C_o \operatorname{erf}[x/2(Dt_e)^{1/2}] . \tag{5}$$

This gives the aging curves which show that on cessation of charging, the front of the profile continues spreading inwards but the deuterium in the immediate surface layers escapes to the atmosphere; the maximum concentration declines and moves inwards. Only for very long charging times compared with release times is the maximum concentration, approximately equal to the original immediate sub-surface concentration, $C_o$. Because of the delay between charging and measurement in the present work, deuterium release is significant. Nevertheless, $C_o$ can be extracted by normalizing Eq. 5 to the measured profile.

An example of results for the analytic method is given in Fig. 2 for a specimen electrocharged for $6 \times 10^3$ s and probed 660 s later. Note that the specimen surface is at the right-hand side in the yield/channel plot and at the left-hand side of the concentration-depth plot. A value of $\sqrt{Dt} = 0.28\ \mu m$ gives the closest fit to the data and provides the concentration-depth curve in the upper part of the figure. This curve is for an aging period of 660 s, and this is reflected in the curve at shallow depths, <0.5 μm, where much of the deuterium has escaped.

When the deconvolution method is used, the resulting C(first-order approximation) becomes the first trial function which is then renormalized to fit the yield data (more exactly, a second-order approximation). Concentration profiles obtained this way for the aged specimens are given in Fig. 3.

These ion beam measurements are quantitative in concentration and depth to an accuracy of 5–20%.

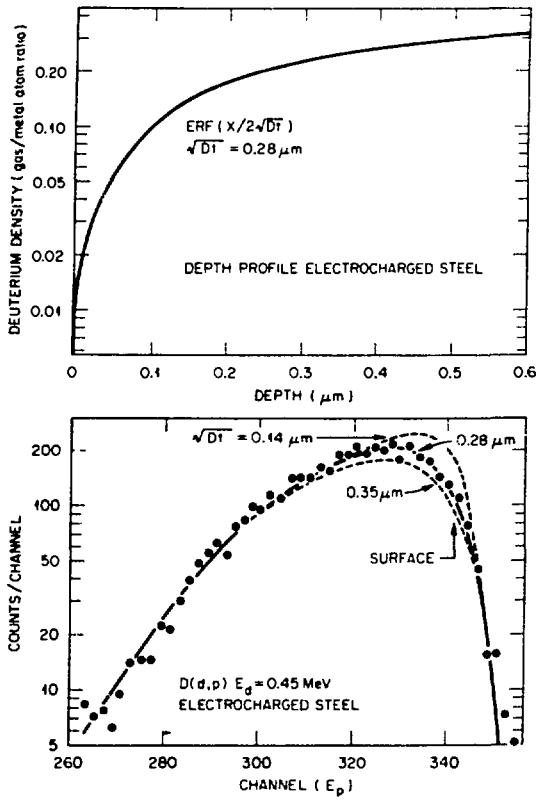


Fig. 2 - Data and calculated fits for a D(d,p)T reaction spectrum from a 0.45-MeV deuterium beam incident on 310 stainless steel electrocharged with deuterium for 100 min and aged 11 min before probing. The corresponding concentration profile is shown above the data. The right-hand edge of the spectrum corresponds to the surface of the specimen.

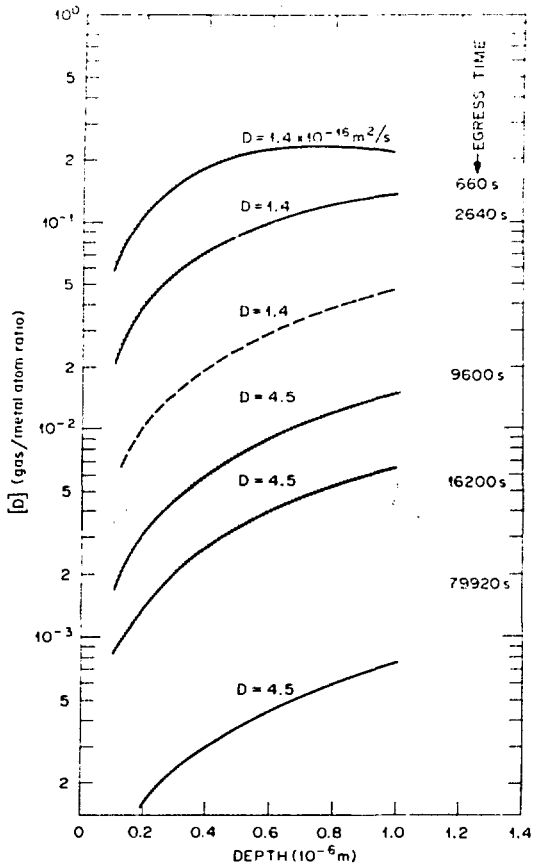


Fig. 3 - Deuterium depth profiles as a function of egress time following a 100 min electrocharge. Data shown hatched to indicate uncertainty.

## Diffusion Coefficient

The best-fit value of $\sqrt{Dt}$ = 0.28 μm for Fig. 2 gives a diffusion coefficient for deuterium in austenite at 25°C of $1.4 \times 10^{-15}$ $m^2s^{-1}$. This is based on the assumption that the initial deuterium concentration ($t_e = 0$) in Fig. 1 is uniform so that the analytic form $\mathrm{erf}(x/2\sqrt{Dt})$ is an appropriate description of the concentration profile. While this may be satisfactory for short aging times, it will not be valid at longer times, $t_e \gtrsim 10^3$ s, and the diffusion equations must be solved more exactly to portray the true deuterium loss. To do this we substitute

$$C(x,t_e = 0) = C_o \,\mathrm{erfc}[x/2(Dt_i)^{1/2}] \; . \qquad (6)$$

With this condition, we have solved numerically the equation

$$\frac{\partial C}{\partial t} = D \frac{\partial^2 C}{\partial x^2} , \qquad (7)$$

assuming the same diffusion constant for ingress and egress.

The solutions were obtained with the use of the differential equation solver GEARB (15), utilizing 150 grid points. The boundary condition $\partial c/\partial x=0$ was applied at an internal point of 12 μm, sufficiently deep for the longest times to avoid interference in the 0–1 μm region from any "back reflected" deuterium. The corresponding diffusion coefficients are shown on the egress curves in Fig. 3 and are further considered in the discussion section.

## The Initial Deuterium Concentration

When the solutions to the differential equation are adjusted to fit the data in Fig. 3, two parameters, $C_0$ and D are determined. The overall normalization is $C_0$, the immediate subsurface concentration during electrocharging. This parameter is of special interest because it describes the local concentration of deuterium present in the steel during the charging. For the curves in Fig. 3, the appropriate $C_0$ value is 0.50 ± 0.15 gas atoms/metal atom. For Fig. 2, $C_0$ = 0.60 ± 0.15.

## Discussion

This work illustrates the usefulness of nuclear microanalysis to gas/metal studies. In particular, the technique provides fast and quantitative information on near-surface concentrations and migration of hydrogen (deuterium) which is unavailable by other techniques. We find that the concentration of deuterium introduced into 310 austenitic stainless steel during cathodic electrolysis of sulphuric acid-$D_2$ containing small amounts of arsenic poison is high, about 0.6 deuterium/metal atoms or 37.5 at. %. This is considerably greater than the values of $1 \times 10^{-2}$ (Ref. 16) and $2.5 \times 10^{-2}$ (Ref. 8) hydrogen atoms/metal atoms quoted for bulk analyses of similarly charged materials which do not allow for a nonhomogeneous depth distribution of the hydrogen. However, Smialowski and his colleagues have long claimed high surface concentrations of hydrogen in α-iron (17) and nickel (18); in the latter surface concentrations as high as 0.7 were attained, and an unstable nickel hydride phase was identified (19,20). Other evidence supports high subsurface hydrogen concentrations in austenite charged under cathodic conditions like ours. For example, x-ray measurements show that the γ lattice is significantly expanded (2,6,7); interplanar spacings are reversibly increased by about 5% (Ref. 7). When this increase is compared with the linear increase in the host unit cell with hydrogen concentration in other single-phase fcc materials charged in high-pressure gaseous hydrogen (21), it corresponds to a hydrogen/metal ratio of 0.62. Also, the calculations and experiments of Atrens et al. (22) on rates of ingress and egress of cathodic hydrogen in 310 steel, indicate a subsurface hydrogen concentration of about unity. Our measurements confirm these high hydrogen levels. We have also done transmission electron microscopy studies of these specimens and find that there was dense microstructural damage created in the surface layers of our specimens. Details of this damage will be made available elsewhere. Briefly, the damage consisted of intense bands of dislocations and faults on slip planes, with cracks at a few of the slip bands and at some annealing twins, grain boundaries, and inclusions. The cracks were barely discernible by optical metallography but were easily revealed by electron microscopy. This damage commenced in very short charging times

as dislocation loops emanating from the specimen surface and later from interfaces. With increasing charging time the damage moved slowly inwards as a front. In 24 h it penetrated only $\sim 5 \times 10^{-6}$ m; serial sectioning and further deuterium profiling showed that the deuterium concentration also declined beyond this depth. We note, too, that if we use our extracted diffusion coefficient of $1.4 \times 10^{-16}$ $m^2s^{-1}$, the penetration depth for a 24-h charge given by $x = \sqrt{Dt}$ is about $4 \times 10^{-6}$ m. Charging in unpoisoned electrolyte, which induced lower deuterium levels, caused relatively little damage. The implication is that the near-surface damage structure resulted from the deuterium content or gradient exceeding some critical value in those regions. Such structures could develop from stress relief by dislocation generation and shear at steep deuterium gradients between a near-surface metal lattice expanded by deuterium and a relatively unexpanded substrate lattice.

In the light of these findings, it is reasonable to suppose that the plastic deformation, martensite formation and cracking observed by others (2–8) at the free surface of austenite after cathodic hydrogenation in poisoned electrolyte were also caused by very high hydrogen concentrations similar to those measured here. These "skins" of damage may contribute to the reported hydrogen embrittlement of 310 steel. In this alloy hydrogen embrittlement is noted only for conditions of cathodic hydrogenation in poisoned electrolyte (2,16,23,24) but not when charging is done in high-pressure hydrogen gas or in unpoisoned electrolyte at 280°C (28).

The diffusion coefficients determined from Figs. 2–3 are in agreement with the extrapolated values for a range of austenitic stainless steels (Table I) at 25°C. This suggests that most of the deuterium remains in atomic form even at concentrations of several atomic percent. A small isotope dependence is consistent throughout the table. Agreement with the literature despite the intense dislocation damage in our measurement area implies that the dislocations are not interfering with the migration of the deuterium at high concentrations. We take this to mean that there is sufficient deuterium present to saturate any trapping sites presented by the dislocations and to leave most deuterium free to migrate. The amount of cracking observed by TEM is not enough to seriously affect diffusion.

Table I. Comparison of Diffusion Coefficients of Hydrogen and Its Isotopes in Austenitic Stainless Steels at 298 K

| Type Steel | Isotope | Measurement Temperature Range (K) | D (298 K) ($\times 10^{-16}$ $m^2/s$) | Reference |
|---|---|---|---|---|
| 316, 304 | T | 298–498 | 0.96 | 29 |
| 310, 309, 304 | D | 385–713 | 1.6 | 30 |
| 310 | H/D | 472–779 | 13.8/11.6 | 31 |
| 309 | H/D | 423–873 | 2.9/2.1 | 32 |
| 304 | T | 373–573 | 1.32 | 33 |
| 310 | D | 298 | 1.4 ± 0.2 | this work $C_0 \approx 0.10$ |
| | | | 4.2 ± 1.0 | this work $C_0 \lesssim 0.01$ |

Other sources of interference might arise from barriers at the free surface, and from deuterium interaction with impurities and with other deuterium atoms. We looked for evidence of deuterium blocked at the surface and found only very slight amounts. Interference by other impurities, if it occurred, is likely to be common to all the measurements in the table, so it would not show as a discernible difference in our value. We did find signs of a possible interaction between the deuterium atoms, as follows. When the diffusion coefficient of $1.4 \times 10^{-16}$ $m^2s^{-1}$ was applied to the set of curves in Fig. 3, good fits were obtained for the $t_e$ = 660 s and 2640 s aging curves, but not for the curves for longer aging times. To fit the $t_e$ = 9600 s and 16,200 s data, it was necessary to *increase* the diffusion coefficient by a factor of three. At these aging times the deuterium levels were also considerably lower than for the shorter times. Such an increase in diffusivity with decreasing concentration is observed in other hydrogen-metal systems, as recently summarized by Volkl and Alefeld (34). The explanation is that the effective diffusion coefficient has a concentration dependence through the activity coefficient, $\gamma$, thus (35)

$$D = D^* \; [1 + \partial(\ln\gamma)/\partial(\ln C)] \; . \qquad (8)$$

With increasing concentration, the mutual interaction of atomic hydrogen in a metal will lower its activity coefficient thus lowering the hydrogen diffusivity D compared to the infinitely dilute case D* (sometimes referred to as the "tracer" or Einstein diffusion coefficient).

At the longest aging time ($8 \times 10^4$ s) and corresponding low concentrations ($\lesssim 10^{-3}$), we find the amount of residual deuterium is somewhat higher than predicted. The most reasonable explanation of this is that at these low deuterium concentrations transitory trapping by the dislocation damage structure is being observed.

## Conclusions

1. Nuclear microanalysis is a useful and fast technique for studying the distribution and migration of deuterium (hydrogen) in metals.

2. The near surface concentration of deuterium introduced into 310 austenitic stainless steel during cathodic charging in sulphuric acid-$D_2$ poisoned with 2.5 mg/l arsenic at 24°C is 0.6 deuterium atoms per metal atom.

3. Concurrent with this high deuterium concentration, intensive microstructural damage is developed in the form of dislocations and cracks.

4. Egress of deuterium after charging does not appear to be affected by the dislocation damage for egress times $\lesssim 10^4$ s (i.e., deuterium $\gtrsim 10^{-2}$) and the diffusion coefficient at 25°C is $1.4 \times 10^{-16}$ $m^2s^{-1}$, for $C \approx 0.10$.

5. At longer egress times (and lower deuterium content), the effective diffusion coefficient is increased threefold, compatible with a concentration dependence of the hydrogen activity coefficient.

6. At long egress time and low deuterium level ($\lesssim 10^{-3}$), the residual deuterium is observed to be less mobile as if trapped by dislocations or other defects.

7. Even at high concentrations most of the deuterium remains in atomic form.

## Acknowledgment

We appreciate the assistance of J. T. Houston in these experiments, and the helpful discussions of hydrogen diffusion with L. K. Mansur.

## References

1. F. Eisenkolb and G. Ehrlich, *Archiv. für das Eisenhüttenwesen*, 1954, 3–4, p. 187.
2. M. L. Holzworth and M. R. Louthan, Jr., *Corrosion*, 1968, vol. 24, p. 110.
3. M. L. Holzworth, *Corrosion*, 1969, vol. 25, p. 107.
4. K. Kamachi, S. Miyata, and M. Eto, *Japan Inst. Met.*, 1969, vol. 33, p. 824.
5. H. Okada, Y. Hosoi, and S. Abe, *Corrosion*, 1970, vol. 26., p. 183.
6. K. Kamachi, K. Akiyoshi, and H. Hayashi, paper 2C13 in *Deuxieme Congres International L'Hydrogene Dans Les Metaux*, Paris, 1977.
7. H. Mathias, Y, Katz, and S. Nadiv, *Met. Sci.*, 1978, p. 129.
8. P. Maulik and J. Burke, *Scripta Met.*, 1975, vol. 9, p. 17.
9. W. K. Chu, J. W. Mayer, and M. A. Nicolet, *Backscattering Spectroscopy*, Academic Press, New York, 1978.
10. M. B. Lewis and K. Farrell, in Proc. TMS-AIME Symp., *Advanced Techniques for Characterization of Microstructures*, J. A. Spitznagel and F. W. Wiffen, eds., Las Vegas, February 1980, in press.
11. M. B. Lewis and K. Farrell, *Appl. Phys. Lett.* 1980, vol. 36, p. 819.
12. M. B. Lewis, *Analysis of Nuclear Backscattering and Reaction Data by the Method of Convolution Integrals*, ORNL/TM-6697, Oak Ridge National Laboratory, 1979.
13. H. H. Anderson and J. F. Ziegler, *Hydrogen Stopping Powers and Ranges*, Pergamon Press, New York, 1977.
14. L. Ruby and R. B. Crawford, *Nucl. Instr. Methods* 1963, vol. 24, p. 413; R. B. Theus, W. J. McGarry, and L. A. Beach, *Nucl. Phys.*, 1966, vol. 8, p. 273.
15. A. C. Hindmarsh, *GEARB: Solution of Ordinary Differential Equations Having Banded Jacobians*, UCID-30059, Lawrence Livermore Laboratory, 1975.
16. J. A. Peterson, R. Gibala, and A. R. Troiano, *J. Iron Steel Inst.*, 1969, p. 86.
17. M. Smialowski, *Hydrogen in Steel*, Addison-Wesley, Reading, Mass., and Pergamon Press, New York, 1962.
18. B. Baronowski and M. Smialowski, *Intern. J. Phys. Chem. Solids*, 1959, vol. 12, p. 206.
19. A. Janko, *Bull. Acad. Polon, Sci., Ser. Sci. Chim.*, 1960, vol. 8, p. 131.
20. A. Janko and P. Michel, *Comptes Rendus*, 1960, vol. 251, p. 1001.
21. B. Baronowski, S. Majchrzak, and T. B. Blanagan, *J. Phys. F: Met. Phys.* 1971, vol. 1, p. 258.

22. A. Atrens, J. J. Bellina, N. F. Fiore, and R. J. Coyle, *The Metal Science of Stainless Steels*, p. 54, E. W. Collings and H. W. King, eds., AIME, 1978.

23. M. B. Whiteman and A. R. Troiano, *Corrosion*, 1965, vol. 21, p. 53.

24. M. L. Mehta and J. Burke, *Corrosion*, 1975, vol. 31, p. 108.

25. R. M. Venett and G. S. Ansell, *Trans. ASM*, 1967, vol. 60, p. 242.

26. R. J. Walter and W. T. Chandler, *Mater. Sci, Eng.*, 1971, vol. 8, p. 90.

27. M. R. Louthan, Jr., G. R. Caskey, Jr., J. A. Donovan, and D. E. Rawl,Jr., *Mater. Sci. Eng.*, 1972, vol. 10, p. 357.

28. R. Lagneborg, *J. Iron Steel Inst.*, 1969, p. 363.

29. J. H. Austin, T. S. Ellerman, and K. Verghase, *J. Nucl. Mater.*, 1973, vol. 48, p. 307.

30. M. R. Louthan, Jr., and R. G. Derrick, *Corros. Sci.*, 1975, vol. 15, p. 565.

31. N. R. Quick and H. H. Johnson, *Metall. Trans.*, 1979, vol. 10A, p. 67.

32. W. J. Kass and W. J. Andrzejewski, AEC Report No. SC-DR-72-0137, Washington, 1972, unpublished.

33. K. F. Chaney and G. W. Powell, *Metall. Trans.*, 1970, vol. 1, p. 2356.

34. J. Völkl and G. Alefeld, *Topics in Applied Physics*, vol. 28, p. 321, G. Alefeld and J. Völkl, eds., Springer-Verlag, Berlin and New York, 1978.

35. P. G. Shewman, *Diffusion in Solids*, McGraw-Hill, New York, 1963.